

# Hard-Sphere Heat Conductivity via Nonequilibrium Molecular Dynamics

Karl W. Kratky<sup>1</sup> and William G. Hoover<sup>2</sup>

*Received October 14, 1986; revision received April 7, 1987*

---

We use an Evans-Gillan driving force  $F^d$ , together with isokinetic and isoenergetic constraint forces  $F^c$ , to drive steady heat currents in periodic systems of 4 and 32 hard spheres. The additional driving and constraint forces produce curved trajectories as well as additional streaming and collisional contributions to the momentum and energy fluxes. Here we develop an analytic treatment of the collisions so that the simulation becomes approximately ten times faster than our previous numerical treatment. At low field strengths  $\lambda$ , for  $\lambda\sigma$  less than 0.4, where  $\sigma$  is the hard-sphere diameter, the 32-sphere conductivity is consistent with Alder, Gass, and Wainwright's 108-sphere value. At higher field strengths the conductivity varies roughly as  $\lambda^{1/2}$ , in parallel with the logarithmic dependence found previously for three hard disks.

---

**KEY WORDS:** Nonequilibrium molecular dynamics; heat conductivity; hard spheres.

## 1. INTRODUCTION

Boltzmann formulated the atomistic basis for nonequilibrium flows of mass, momentum, and energy, described by the linear laws of Fick, Newton, and Fourier.<sup>(1)</sup> A general method for expressing the corresponding transport coefficients, the diffusion, viscosity, and heat conductivity, in terms of equilibrium current, stress, and heat current autocorrelation time integrals was developed by Green and Kubo. Alder and Wainwright applied this linear response formalism to the simplest prototypical atomic model, hard spheres, during the period from 1955 to 1970.<sup>(2,3)</sup>

---

<sup>1</sup> Institut für Experimentalphysik, Universität Wien, A-1090 Wien, Austria.

<sup>2</sup> Department of Applied Science, University of California at Davis, and Lawrence Livermore National Laboratory, Livermore, California 94550.

A major accomplishment of the computational effort during this period was establishing the form of the equilibrium equation of state characterizing the number dependence of the pressure<sup>(2,4)</sup> and establishing the location of the fluid–solid phase transition.<sup>(5)</sup> This work led to a fairly reliable method for calculating fluid-phase equilibrium properties by perturbation theory based on the hard-sphere results.<sup>(6)</sup> Nonequilibrium progress has been more difficult, primarily due to the lack of a useful perturbation theory. The Green–Kubo method provided a route to the linear transport coefficients using equilibrium molecular dynamics. Because the calculations were time-consuming, being based on the analysis of fluctuations, and showed considerable number dependence, there was motivation to develop alternative approaches.<sup>(7,8)</sup>

New methods began to be developed for treating nonlinear transport, using driving forces and constraint forces to produce fluxes under steady-state, far-from-equilibrium conditions. By 1982 Evans and Gillan had shown that heat flow, the transport property studied here, could be induced by using a driving force depending on individual particle contributions to the energy and pressure tensor.<sup>(9,10)</sup> Their idea has been applied to both soft<sup>(11,12)</sup> and hard<sup>(13)</sup> spheres. Heat flow requires a system of three or more particles and is intrinsically more complex than diffusive or viscous flows, for which two particles suffice.<sup>(14)</sup> Here we apply the Evans–Gillan idea to hard spheres.

The present work is organized as follows. In Section 2 we give a brief resume of the Evans–Gillan recipe for the determination of the heat conductivity. In Section 3 we describe an analytic method which makes the collisional calculation more efficient than the purely numerical approach followed previously,<sup>(13)</sup> particularly for dense fluids and for solids. Conductivity results based on this analytic approach are listed in Section 4. Section 5 is a discussion.

## 2. BASIC EQUATIONS

In the interest of generality and clarity, we first consider a continuous, pairwise-additive, spherically symmetric interaction potential. We consider later the hard-sphere limit. The periodic system, which can be fluid or solid, with volume  $V$ , contains  $N$   $D$ -dimensional particles of mass  $m$ . The total momentum of the system is zero. Particle  $i$ , located at  $\mathbf{r}_i$ , has momentum  $\mathbf{p}_i$ . The total energy  $E$  is a sum of kinetic and potential contributions  $K$  and  $\Phi$ :

$$E = K + \Phi = \sum p_i^2 / (2m) + \sum \sum \phi_{ij}(r_{ij}) \quad (1)$$

$$\mathbf{r}_{ij} \equiv \mathbf{r}_i - \mathbf{r}_j, \quad r_{ij} \equiv |\mathbf{r}_{ij}|$$

The single sum runs over all  $N$  particles. The double sum includes all pairs of particles. Three types of forces act on each particle  $i$ : An *applied* force  $\mathbf{F}_i^a = \mathbf{F}_i$  from the potential gradient, an external *driving* force  $\mathbf{F}_i^d$  inducing, on the average, a heat flow in the  $x$  direction, and a *constraint* force  $\mathbf{F}_i^c$  fixing either the total energy  $E$  or the kinetic energy  $K$ :

$$\begin{aligned}\dot{\mathbf{p}}_i &= d\mathbf{p}/dt = \mathbf{F}_i + \mathbf{F}_i^c + \mathbf{F}_i^d, & 1 \leq i \leq N \\ \mathbf{e}_{ij} &= \mathbf{r}_{ij}/r_{ij} \\ \mathbf{F}_i &\equiv \sum_j \mathbf{F}_{ij} = -\sum_j (d\phi_{ij}/dr_{ij}) \mathbf{e}_{ij} & (2) \\ F_{\alpha i}^d &\equiv \lambda(\delta_{\alpha x} \Delta E_i + \Delta P_{\alpha x, i}^\phi V), & \alpha = x, y, \dots \\ \mathbf{F}_i^c &\equiv -\zeta_E \mathbf{p}_i \quad \text{or} \quad -\zeta_K \mathbf{p}_i\end{aligned}$$

$\Delta E_i$  indicates the actual instantaneous energy for particle  $i$ ,  $E_i$ , minus the average energy per particle,  $E/N$ , at the same time:

$$\Delta E_i = \left[ p_i^2/(2m) + \frac{1}{2} \sum \phi_{ij} \right] - [E/N] \quad (3)$$

The sum runs over all particles  $j$  interacting with  $i$ . Similarly, the individual-particle fluctuations in potential pressure-tensor components,

$$\Delta P_{\alpha x, i}^\phi = P_{\alpha x, i}^\phi - [P_{\alpha x}^\phi/N] \quad (4)$$

follow from the definition of the instantaneous pressure tensor:

$$P_{\alpha\beta} V = P_{\alpha\beta}^K V + P_{\alpha\beta}^\phi V = \sum p_\alpha p_\beta / m + \sum \sum r_{\alpha, ij} F_{\beta, ij} = \sum P_{\alpha\beta, i} V \quad (5)$$

Note that only the potential part  $P^\phi$  of the pressure tensor contributes to the driving force  $F^d$ . This force is constructed so as to induce a mean heat flux in the  $x$  direction with the resulting dissipation matching that from irreversible thermodynamics.<sup>(9)</sup> The instantaneous heat flux  $\mathbf{Q}$  is given by

$$m\mathbf{Q}V = \sum \mathbf{p}_i E_i + \sum \sum \mathbf{r}_{ij} \left[ \frac{1}{2} (\mathbf{p}_i + \mathbf{p}_j) \cdot \mathbf{F}_{ij} \right] \quad (6)$$

In the constraint force  $\mathbf{F}^c$ , the “friction” coefficient  $\zeta_E$  or  $\zeta_K$  is a function of time, but has the same value for all particles.  $\zeta$  is chosen so that either the total energy  $E$  or the kinetic part  $K$  is a constant of motion. The two

choices will be called "isoenergetic" and "isokinetic," respectively. Explicit construction of  $\zeta$  yields<sup>(11)</sup>

$$\zeta_E = \lambda Q_x V / (2K), \quad \zeta_K = \zeta_E + \left[ \sum \mathbf{p}_i \cdot \mathbf{F}_i / (2Km) \right] \quad (7)$$

for the isoenergetic and isokinetic cases, respectively. One can see that for absent driving force ( $\lambda = 0$ ),  $\zeta_E$  is also vanishing. This corresponds to the usual Newtonian equilibrium molecular dynamics. In  $\zeta_K$ , however, there is an extra term independent of  $\lambda$ . Thus, even for  $\lambda = 0$ , the isokinetic molecular dynamics is non-Newtonian.<sup>(13)</sup>

Measuring the heat flux  $\mathbf{Q}$  makes it possible to obtain the thermal conductivity  $\kappa$  from the relation<sup>(11)</sup>

$$\bar{Q}_x = \kappa \lambda T \quad (8)$$

The bar means time average.  $T$  is the absolute temperature defined by the relation

$$\bar{K} = \frac{1}{2} DNkT \quad (9)$$

where  $k$  is Boltzmann's constant.

Equation (8) may be used for *any*  $\lambda$  to define formally a non-equilibrium  $\kappa = \kappa(\lambda)$ . To compare with linear Green-Kubo results,<sup>(3)</sup> however, small  $\lambda$ 's have to be used. Equation (8) may be compared with Fourier's law:

$$\mathbf{Q} = -\kappa \nabla T \quad (10)$$

which likewise defines a constant  $\kappa$  (linear regime) only for small temperature gradients.

Both  $\bar{Q}_x$  and  $\kappa$  depend on  $N$ . For  $N = 2$ , the heat flux vanishes, since  $\mathbf{p}_2 = -\mathbf{p}_1$ ; compare (6). One might conjecture that  $\kappa$  is a monotonically increasing function of  $N$  up to the thermodynamic limit. The form of this number dependence was discussed, qualitatively, in Ref. 3.

The meaning of *temperature* for small systems was discussed in Ref. 15. We use temperature in the sense of  $\tilde{T}$  of that reference, generalized to nonequilibrium systems. Furthermore, the thermodynamic *pressure* in  $D$  dimensions is given by the usual relation

$$P = \sum_{\alpha} \bar{P}_{\alpha\alpha} / D \quad (11)$$

### 3. CALCULATION METHOD

#### 3.1. Streaming Motion ( $\Phi = 0$ )

We consider soft, repulsive, spherical particles of diameter  $\sigma$ , with the interaction potential vanishing for  $r \geq \sigma$ . If no pair of particles overlaps, then  $\phi = 0$ , and the isoenergetic and isokinetic cases coincide. The corresponding "streaming motion" is characterized by

$$\begin{aligned} dp_{\alpha i}/dt &= \lambda \delta_{\alpha x} (\Delta K_i) - \zeta p_{\alpha i} \\ \zeta &= \lambda \sum p_{xi} K_i / (2K_m) \end{aligned} \quad (12)$$

$K_i$  and  $\Delta K_i$  appear, rather than the  $\Delta E_i$  of (2) and (3), because the potential vanishes between collisions. The  $ND$  equations of motion are coupled by  $\zeta$ . Equations (5) and (6) are simplified:

$$P_{\alpha\beta} V = \sum p_{\alpha i} p_{\beta i} / m \quad (13)$$

$$mQV = \sum \mathbf{p}_i K_i = \sum \mathbf{p}_i \Delta K_i \quad (14)$$

for the streaming motion. For hard spheres  $\bar{K} = K^{\text{str}}$  and combining (9), (11), and (13) shows that  $P^{\text{str}} V / NkT = 1$  as in the equilibrium case.

Setting  $\sigma = 0$  yields the ideal gas case. Then *only* streaming motion occurs, which is in general no longer characterized by straight lines if  $\lambda \geq 0$ . Without loss of generality, we assume  $\lambda \geq 0$  in the following. What is the maximum  $Q_x$  that can be achieved for given  $N$ ,  $D$ , and  $kT$  when the center of mass is fixed? A Lagrange-multiplier calculation yields the result that one particle (say particle 1) moves in the positive  $x$  direction. The rest move in the opposite direction:

$$\begin{aligned} \mathbf{p}_i &= -\mathbf{p}_1 / (N-1), \quad 2 \leq i \leq N \\ K &= \frac{1}{2} DNkT = p_1^2 / [2m(1-N^{-1})] \end{aligned} \quad (15)$$

The corresponding heat flux is

$$mQ_x^{\text{max}} V = \frac{1}{2} (1 - 2N^{-1}) [m(DNkT)^3 / (1 - N^{-1})]^{1/2} \quad (16)$$

Thus, the collisionless ideal-gas behavior may be characterized as follows: For small  $\lambda$ ,  $\bar{Q}_x$  increases proportional to  $\lambda$ , as given by (8). If  $\lambda$  becomes very large and if the streaming motion persists for a long time,  $\bar{Q}_x$  tends to a saturation value  $Q_x^{\text{max}}$  given in (16). Accordingly,  $\kappa$  becomes proportional to  $1/\lambda$  for large  $\lambda$ . Between collisions, the streaming motion of the soft,

repulsive spherical particles is the same as that of an ideal gas and can be treated numerically without problems. The streaming motion ends when any pair of particles happens to touch. Without loss of generality, we assume a collision of particles 1 and 2 in the following.

### 3.2. Collisions

In our preliminary calculations in Ref. 13, the colliding motion was treated numerically, assuming potentials proportional to  $(\sigma - r)$  for  $r \leq \sigma$  and vanishing for  $r \geq \sigma$ . The equations of motion were solved for a series of increasing proportionality constants until the "hard-sphere limit" was achieved. Because  $\phi$  was continuous, the motion, pressure, and heat flux vector could all be calculated without trouble. The pressure and heat flux contributions from the collisions are not the same for isoenergetic and isokinetic cases. This comes from the different momentum histories *during* the collision. At the end of the collision (defined by  $r_{12} = \sigma$ ), the *motions coincide* in the two cases. This is because the extra net work performed by the driving force during each collision is exactly offset by the isoenergetic or isokinetic friction coefficient. Thus, the coordinate trajectories are the same in the hard-sphere limit. The numerical calculation of collisions was relatively slow because the momenta of *all* the particles varied with time. In the present paper, we display a theoretical treatment of collisions that substantially reduces this numerical work in the hard-sphere limit. Only two-particle collisions 1–2 have to be considered. During each collision, the product of force and distance greatly exceeds  $kT$ , and the distance vector  $\mathbf{r}_{12}$  is essentially given by  $\hat{\mathbf{r}}_{12}$ , the vector at the beginning of collision. Retaining the leading terms, Eq. (2) becomes

$$\dot{\mathbf{p}}_i = d\mathbf{p}_i/dt = N_i F_{12} \hat{\mathbf{e}}_{12} - \zeta \mathbf{p}_i, \quad 1 \leq i \leq N \quad (17)$$

where  $\hat{\mathbf{e}}_{12} = \hat{\mathbf{r}}_{12}/\sigma$ , and  $F_{12} = |\mathbf{F}_{12}|$ , the magnitude of the force exerted on particle 1 by particle 2. We have

$$\begin{aligned} N_1 &\equiv 1 + \frac{1}{2}\lambda \hat{x}_{12}(1 - 2N^{-1}) \\ N_2 &\equiv -1 + \frac{1}{2}\lambda \hat{x}_{12}(1 - 2N^{-1}) \\ N_i &\equiv -\lambda \hat{x}_{12}/N, \quad 3 \leq i \leq N \end{aligned} \quad (18)$$

The terms linear in  $\lambda$  come from the driving force. The general solution of (17) is

$$\begin{aligned} \mathbf{p}_i(t) &= [I(t)]^{-1} \left[ \hat{\mathbf{p}}_i + \hat{\mathbf{e}}_{12} N_i \int_0^t F_{12}(t') I(t') dt' \right] \\ I(t) &= \exp \int_0^t \zeta(t') dt', \quad \hat{\mathbf{p}}_i \equiv \mathbf{p}_i(0), \quad \hat{\mathbf{e}}_{12} \equiv \hat{\mathbf{e}}_{12}(0) \end{aligned} \quad (19)$$

with zero indicating the time at the beginning of collision. This solution, however, can only be used if  $\zeta$  is known as a function of  $t$ . The friction coefficients that couple the  $ND$  differential equations are given by (7) as follows:

$$\zeta_E = F_{12} [\frac{1}{2} \lambda \hat{x}_{12} (\mathbf{p}_1 + \mathbf{p}_2)] / (2Km) \quad (20)$$

$$\zeta_K = F_{12} [\frac{1}{2} \lambda \hat{x}_{12} (\mathbf{p}_1 + \mathbf{p}_2) + (\mathbf{p}_1 - \mathbf{p}_2)] / (2Km) \quad (21)$$

It is convenient to use the notation  $\mathbf{p}_{12} \equiv \mathbf{p}_1 - \mathbf{p}_2$  and  $\mathbf{s}_{12} \equiv \mathbf{p}_1 + \mathbf{p}_2$  for the relative and total momenta of the colliding pair. Then (17) and (18) yield

$$\dot{\mathbf{p}}_{12} = 2\mathbf{F}_{12} - \zeta \mathbf{p}_{12} \quad (22)$$

$$\dot{\mathbf{s}}_{12} = \lambda x_{12} (1 - 2N^{-1}) \mathbf{F}_{12} - \zeta \mathbf{s}_{12} \quad (23)$$

Projection onto  $\hat{\mathbf{e}}_{12} = \hat{\mathbf{r}}_{12}/\sigma$ , indicated by a prime, gives

$$\dot{p}'_{12} = 2F_{12} - \zeta p'_{12} \quad (24)$$

$$\dot{s}'_{12} = [\lambda \hat{x}_{12} (1 - 2N^{-1})] F_{12} - \zeta s'_{12} \quad (25)$$

where  $F_{12}$  is a steep repulsive force yet to be chosen explicitly.

The isoenergetic case is characterized by

$$\zeta_E = F_{12} [\frac{1}{2} \lambda \hat{x}_{12} s'_{12}] / (2Km) \quad (26)$$

$$(\dot{E} = 0) \rightarrow (\dot{K} = -\dot{\Phi} = F_{12} p'_{12}/m)$$

The isokinetic case is given by

$$\zeta_K = F_{12} [\frac{1}{2} \lambda \hat{x}_{12} s'_{12} + p'_{12}] / (2Km) \quad (27)$$

$$(\dot{K} = 0) \rightarrow (K = \text{const})$$

Thus, the isoenergetic case has been reduced to three coupled differential equations in the variables  $p'_{12}$ ,  $s'_{12}$ , and  $K$ . The isokinetic case has been reduced to two coupled equations in the variables  $p'_{12}$  and  $s'_{12}$ . Because this is simpler, the isokinetic case will be solved first.

Having the solution for  $p'_{12}$ ,  $s'_{12}$ ,  $K$  means first knowing  $\zeta$ . See (26) and (27). Then the momenta  $\mathbf{p}_i$  during the collision can be calculated using (19).

Furthermore, the instantaneous pressure and heat flux follow from (5) and (6):

$$P_{\alpha\beta} V = F_{12} \sigma \hat{e}_{\alpha,12} \hat{e}_{\beta,12} \quad (28)$$

$$mQ_{\alpha} V = \frac{1}{2} F_{12} \sigma \hat{e}_{\alpha,12} s'_{12} \quad (29)$$

Generally, each collision begins with  $p'_{12} < 0$  and ends with  $p'_{12} > 0$ . The turning point is given by  $p'_{12} = 0$ . The condition ending the collision is  $\int p'_{12} dt = 0$ . The isokinetic and isoenergetic cases are solved in Appendices A and B, respectively. For the most part, the solution is analytical. Only one-dimensional numerical integrals occur.

#### 4. COMPUTER EXPERIMENTAL RESULTS

In Section 3 and Appendices A and B, the collisions are reduced to one-dimensional quadratures. The solutions were built into the existing computer program,<sup>(13)</sup> which can treat one-, two-, three-, and four-dimensional systems. A series of test runs showed that the reduction in computer time used varies with the number of particles, dimensionality, and density, but is typically a factor ten. For very low densities, where streaming motion is dominant, the gain is only about a factor of two.

In this paper, results for hard spheres are presented. The following particle numbers and densities were investigated:

$$\begin{array}{ll}
 (N = 4, V/V_0 = 1.25), & (N = 32, V/V_0 = 1.25) & \text{typical solid} \\
 (N = 4, V/V_0 = 1.80), & (N = 32, V/V_0 = 1.80) & \text{dense fluid} \\
 (N = 4, V/V_0 = 3.00) & & \text{dilute fluid}
 \end{array} \quad (30)$$

$V_0$  is the close-packed volume  $N\sigma^3/\sqrt{2}$ . For each of the five series of computer experiments,  $(\lambda\sigma)^{1/2}$  was varied between 0.0 and 2.0 in steps of 0.1. The starting configuration was always an fcc structure. Test runs showed that a steady state was achieved after a few hundred collisions in the worst case. For calculating thermodynamic properties, there is the possibility to use one long trajectory or several shorter ones with different (random) initial particle velocities. The second procedure samples the phase space more efficiently.<sup>(16)</sup> Furthermore, calculation of statistical errors is simplified, the mean values due to the simple trajectories being the input data for estimating a quantity and its error. Thus, for given  $N$ ,  $V$ , and  $\lambda$  several trajectories were used. The first 500 collisions of each were thrown away, the consecutive 2500 collisions being utilized for calculation. More details are given in Table I. The quantities calculated are shown in Table II.

Apart from the heat flux data, the results for  $\bar{t}^{\text{str}}$ ,  $Z_E$ , and  $(Z_K - 1)/(Z_E - 1)$  are also presented.  $\bar{t}^{\text{str}}$  is the average time between collisions and  $Z$  is the compressibility factor  $PV/NkT$ . To simplify the presentation of the results, all quantities are displayed in units of  $m$ ,  $\sigma$ , and

Table I. Number of Trajectories and of Collisions for Given  $N$ ,  $V$ , and  $\lambda$  As a Function of  $\lambda^a$

$(\lambda\sigma)^{1/2}$	Number of trajectories	Number of collisions
0.0-0.2	24	60,000
0.3	20	50,000
0.4	16	40,000
0.5	12	30,000
0.6-2.0	8	20,000

<sup>a</sup> Each trajectory started from an fcc lattice with different random initial velocities. The first 500 collisions were used for equilibration, the consecutive 2500 for calculation.

$kT$ . This means that the following symbols (left-hand side) should be read as dimensionless quantities (right-hand side):

$$\begin{aligned}
 \lambda &\rightarrow \lambda\sigma \\
 \bar{t}^{\text{str}} &\rightarrow \bar{t}^{\text{str}}(kT/m)^{1/2} \sigma^{-1} \\
 \bar{Q}_{x,E} &\rightarrow \bar{Q}_{x,E}(kT)^{-3/2} m^{1/2} \sigma^D \\
 (\kappa/k) &\rightarrow (\kappa/k)(kT/m)^{-1/2} \sigma^{D-1}
 \end{aligned} \tag{31}$$

with  $D = 3$  for hard spheres.  $Z$  is already dimensionless.

For  $\lambda = 0$  (i.e., equilibrium), it is possible to compare  $\bar{t}^{\text{str}}$  and  $Z_E$  with values given in Ref. 2, where the same particle numbers and densities occur. The check of consistency is successful, bearing in mind that in Ref. 2 the

Table II. Calculated Quantities, in Units of  $m$ ,  $\sigma$ , and  $kT^a$

$\bar{t}^{\text{str}}$	Average time of streaming motion (between collisions); inverse of the collision rate $\Gamma$
$Z_E$	Compressibility factor $P_E V/NkT$ for the isoenergetic case, calculated from the pressure tensor
$\bar{Q}_{x,E}$	Average heat flux in the $x$ direction (isoenergetic case)
$\kappa_E/k$	Total heat conductivity over $k$ (isoenergetic case)
$\kappa^{\text{str}}/k$	Contribution of streaming motion to the heat conductivity
$(Z_K - 1)/(Z_E - 1)$	Ratio of isokinetic to isoenergetic for the collisional part of the pressure
$\kappa_K^{\text{coil}}/\kappa_E^{\text{coil}}$	Ratio of isokinetic to isoenergetic for the collisional part of $\kappa$

<sup>a</sup> See (31).

number of collisions was low (2000 for  $N=4$ ). For equilibrium hard spheres,

$$Z_E = 1 + \pi^{1/2} / (3N\bar{t}^{str} a_N)$$

$$a_N \equiv (1 - N^{-1}) (\frac{3}{2}N)^{1/2} \Gamma(\frac{3}{2}[N-1]) / \Gamma(\frac{3}{2}N-1) \quad (32)$$

$$a_4 = 0.8904, \quad a_{32} = 0.9869$$

$\Gamma(m)$  is the usual  $\Gamma$ -function,  $(m-1)!$  for positive integral values of  $m$ . In Ref. 2,  $a_N$  (called  $R$  there) was determined experimentally. The theoretical explanation for this correction was given in Refs. 4 and 17. Thus, there is a further check of consistency: One has to compare  $Z_E$  calculated directly from the pressure tensor with  $Z_E$  calculated indirectly via  $t^{str}$ . For small  $\lambda$ , the agreement is perfect. For higher  $\lambda$  (starting at about  $\lambda^{1/2} = 0.7$ ), the deviations become pronounced, indicating nonlinear nonequilibrium behavior.

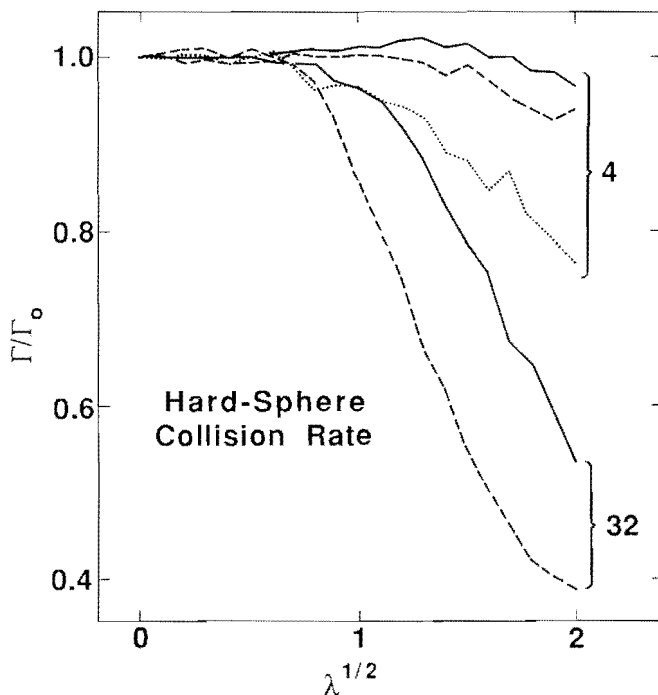


Fig. 1. Variation of the hard-sphere collision rate, relative to the zero-field limit, with field strength. Results for  $V/V_0 = 1.25, 1.80, \text{ and } 3.00$  are indicated with solid, dashed, and dotted lines, respectively.

The detailed results of the computer experiments are exhibited in Appendix C, Tables III–VII. To see the main features, it is more convenient to look at a different representation, Figs. 1–5. Figure 1 shows  $\Gamma = 1/t^{\text{str}}$ , Fig. 2 displays  $Z_E$ . Both quantities do not depend significantly on  $\lambda$  up to  $\lambda^{1/2} = 0.6$ . Thus, for convenience,  $\Gamma$  and  $Z_E$  are divided by their weighted mean ( $0 \leq \lambda^{1/2} \leq 0.6$ ),  $\Gamma^*$  and  $Z_E^*$ , respectively. For higher  $\lambda$ , there are systematic deviations that are not easy to explain theoretically.

The ratio  $(Z_K - 1)/(Z_E - 1) = p_K^{\text{coll}}/p_E^{\text{coll}}$  has been included for the following reason. In Appendix D, it is shown that for  $\lambda = 0$  this quantity is

$$(Z_K - 1)/(Z_E - 1) = 1 - [D(N - 1)]^{-1}, \quad D \geq 1, \quad N \geq 2 \quad (33)$$

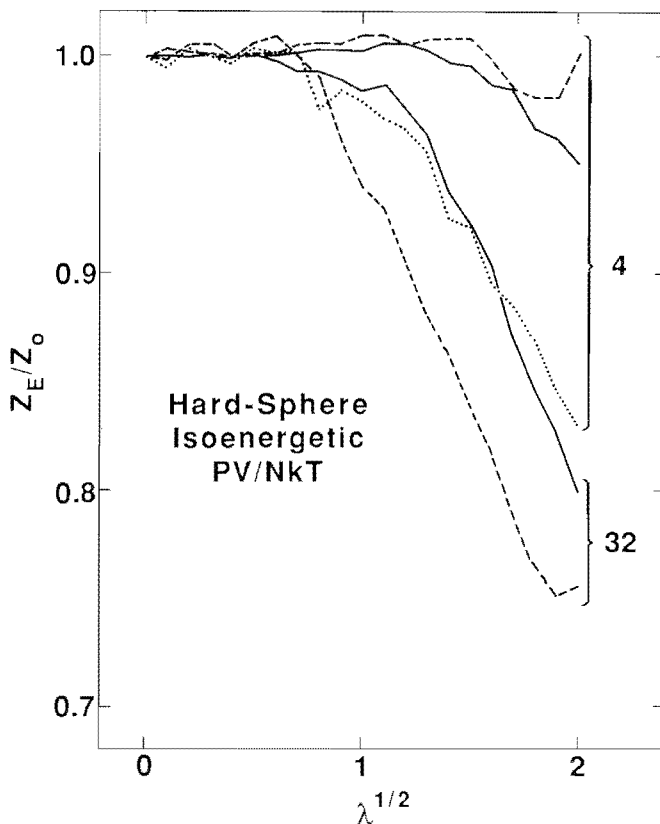


Fig. 2. Variation of the isoenergetic compressibility factor, relative to the zero-field limit, with field strength. Results for  $V/V_0 = 1.25, 1.80,$  and  $3.00$  are indicated with solid, dashed, and dotted lines, respectively.

for  $N$   $D$ -dimensional hard spheres, *independent of density*. The three-dimensional values for  $N=4$  and  $N=32$  are 1.125 and 1.011, respectively. Figure 3 confirms this result for small  $\lambda$ . Compare Tables III–VIII.

For  $D=1$  and  $N=2$ ,  $(Z_K-1)/(Z_E-1)$  becomes infinite. On the other hand,  $(Z_K-1)/(Z_E-1)$  converges to 1 in the thermodynamic limit. This is one feature of a general observation: For hard spheres, the isoenergetic and isokinetic cases both converge to the same thermodynamic limit. This can easily be seen by the following argument: the “typical” potential energy  $\phi_{12}$  during the collision (in the case of very steep soft potentials) is essentially  $kT$ , independent of  $N$ . Thus, the relative contribution of  $\phi_{12}$  to the total energy  $E$  becomes smaller as  $N$  increases:

$$E = K + \phi_{12} \quad (34)$$

$K$  is proportional to  $N$ . The restrictions of constant *total* energy and constant *kinetic* energy become identical if  $N \rightarrow \infty$ .

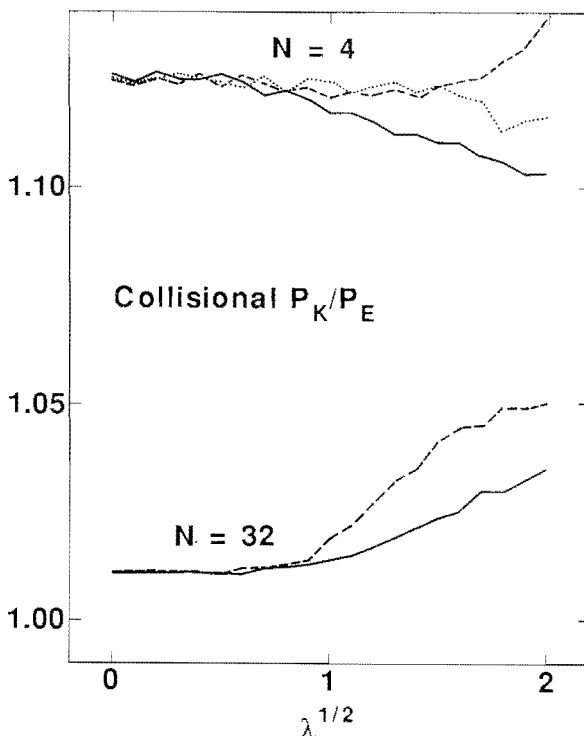


Fig. 3. Variation of the collisional parts of the pressure with field strength. Results for  $V/V_0=1.25, 1.80,$  and  $3.00$  are indicated with solid, dashed, and dotted lines, respectively.

Now we turn to the heat flux. Because  $\bar{Q}_{x,E}$  becomes proportional to  $\lambda$  for small  $\lambda$ , while its fluctuations do not diminish, the statistical accuracy of this quantity becomes poor. This is why we chose to examine more collisions for small  $\lambda$ , as shown in Table I. For  $\lambda^{1/2} = 0.1$ , however, the heat flux data were meaningless, with estimated errors as large as the mean value itself. From heat flux, the corresponding heat conductivities can be calculated using (8). The values of  $\kappa_E$  and its streaming part  $\kappa^{\text{str}}$  are included in Tables III–VIII. Compare Fig. 4. These quantities are highly correlated. Again, no significant dependence on  $\lambda$  can be detected up to  $\lambda^{1/2} = 0.6$ . Thus, one can conclude that linear heat transport is approximately valid in this region. We have used the weighted mean of the results for  $0.2 \leq \lambda^{1/2} \leq 0.6$  as estimates for the equilibrium linear heat conductivity. Table VIII shows these results together with the weighted means

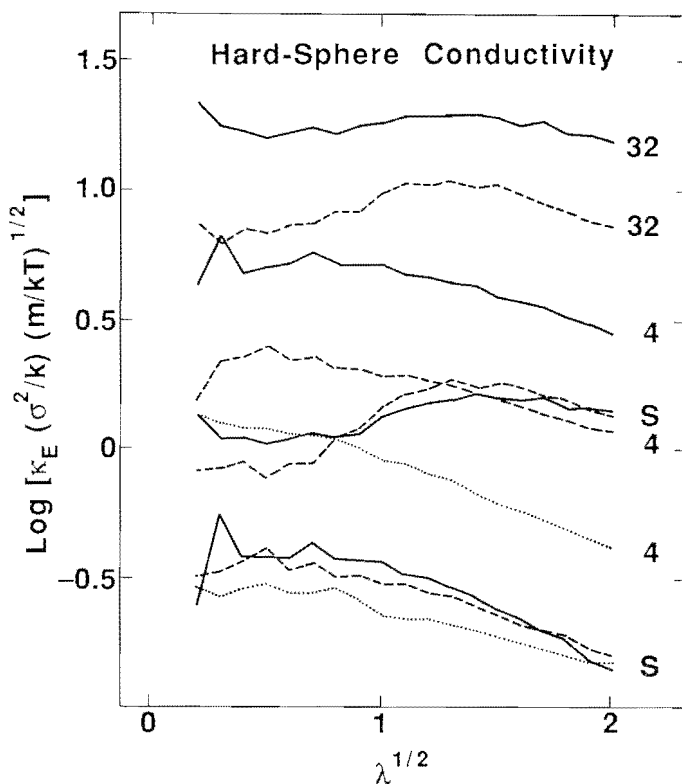


Fig. 4. Variation of conductivity with field strength. Both the total conductivity and the streaming contribution (indicated by S) are shown. Results for  $V/V_0 = 1.25, 1.80,$  and  $3.00$  are indicated with solid, dashed, and dotted lines, respectively.

of  $\bar{t}^{\text{str}}$  and  $Z_E$  for  $0.0 \leq \lambda^{1/2} \leq 0.6$ . As expected,  $\kappa_E$  for  $N=4$  is smaller than for  $N=32$ . A comparison with Ref. 3 is also possible, where  $\kappa_E$  was calculated using the Green-Kubo equilibrium autocorrelation approach:

$$\begin{aligned} V/V_0 = 1.8, \quad N = 108: \quad \kappa_E/k &= 6.94 \pm 0.14 \\ V/V_0 = 3.0, \quad N = 108: \quad \kappa_E/k &= 1.92 \pm 0.02 \end{aligned} \quad (35)$$

One can see that for  $V/V_0 = 1.8$  the result of Ref. 3 and  $\kappa_E/k = 6.79 \pm 0.21$  (Table VIII,  $N=32$ ) are consistent. Thus, the  $N$  dependence is small for  $N$  greater than 32. For comparison, the Enskog  $\kappa_E/k$  ( $V/V_0 = 1.8$ , thermodynamic limit) is 6.74,<sup>(3)</sup> which is close to the above values.

The results of the case  $V/V_0 = 1.8$ ,  $N=32$ , are also presented in the figure. Compare Table VIII. One can see that the extrapolation to equilibrium by averaging the quantities for  $\lambda^{1/2} \leq 0.6$  makes sense; cf. the horizontal bars. As to  $Z_E$ , at  $\lambda^{1/2} = 0.7$ , there seems to be a sharp transition from horizontal behavior to linear dependence on  $\lambda^{1/2}$ . The anticorrelation of  $Z_E$  and  $\bar{t}^{\text{str}}$  can be understood from Eq. (32), which is approximately valid also in the nonequilibrium case. Furthermore, one can see that the heat conductivity  $\kappa_E$  and its streaming part  $\kappa^{\text{str}}$  are highly correlated. The numbers in brackets refer to the basis  $\lambda^{1/2} \leq 0.7$  instead of  $\lambda^{1/2} \leq 0.6$ . Thus, we are on the safe side when considering averages for  $\lambda^{1/2} \leq 0.6$ . More complicated fits would be too flexible.

While  $\bar{t}^{\text{str}}$  and  $Z_E$  are more accurate close to equilibrium, the opposite is the case for  $\kappa_E$  and  $\kappa^{\text{str}}$ ; see Tables III-VII. Is the jumpiness for small  $\lambda$  beyond statistical expectation? The error in Tables III-VIII denotes standard deviation. Thus, one expects that roughly two-thirds of the error bars of  $\bar{t}^{\text{str}}$ ,  $Z_E$ ,  $\kappa_E/k$ , and  $\kappa^{\text{str}}/k$  (for  $\lambda^{1/2} \leq 0.6$ ) cross the appropriate weighted means (Table VIII). Averaging the results of all cases (30) (Tables III-VII) gives the following fractions:

$$\begin{aligned} \bar{t}^{\text{str}}: & 0.83 (0.75), & Z_E: & 0.63 (0.63) \\ \kappa_E/k: & 0.72 (0.67), & \kappa^{\text{str}}/k: & 0.84 (0.77) \end{aligned} \quad (36)$$

Now we consider the ratio of the collisional parts of the heat conductivities

$$\kappa_K^{\text{coll}}/\kappa_E^{\text{coll}} = (\kappa_K - \kappa^{\text{str}})/(\kappa_E - \kappa^{\text{str}}) \quad (37)$$

for small  $\lambda$ . In parallel to the pressure result (see Appendix D), the conductivity ratio seems to be nearly independent of density. See Fig. 5 and Tables III-VII. We could not find a limiting ( $\lambda=0$ ) formula like (33). In that limit the numerator and denominator of Eq. (37) both vanish.

Finally, consider the heat conductivity for  $\lambda^{1/2}$  greater than 0.6. After a

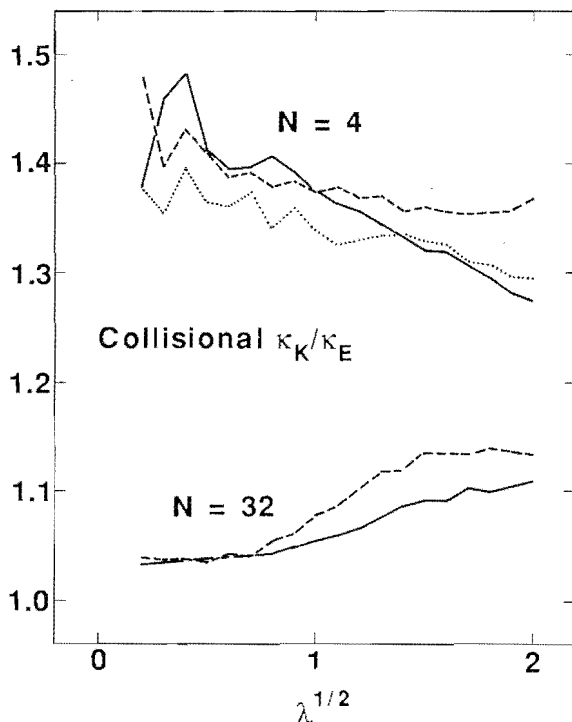


Fig. 5. Ratio of the isokinetic to isoenergetic collisional parts of the conductivity as a function of field strength. Results for  $V/V_0=1.25, 1.80,$  and  $3.00$  are indicated with solid, dashed, and dotted lines, respectively.

transient region,  $\kappa_E$  and  $\kappa^{\text{str}}$  become approximately linearly decreasing functions of  $\lambda^{1/2}$ . This behavior may be compared with Ref. 13, where a system of three hard disks was investigated. There, it turned out that  $\kappa_E$  and  $\kappa^{\text{str}}$  varied linearly with  $\ln \lambda$ . In that case no transient region or "linear regime" could be detected. Obviously, the  $\lambda$  values where these transitions occur are too small to observe in two dimensions, at least with the accuracy obtained in Ref. 13. The three-dimensional case is more favorable. It is indeed possible to get heat conductivities for hard spheres using our method in a reasonable amount of computer time.

## 5. CONCLUSION

The pressures found, in both the fluid and solid phases, agree nicely with those of Alder and Wainwright<sup>(2)</sup> for field strengths below 0.4. In this

region there is negligible coupling, less than 1%, between the heat flux and the pressure tensor.

For the conductivity we find, as suggested by Alder *et al.*,<sup>(3)</sup> considerable number dependence. There is roughly a factor of three between the four-sphere results and the 32-sphere results. The fluid data suggest a conductivity lying near, possibly somewhat below, the Green-Kubo value found for 108 and 500 particles in a dense fluid.

This considerable number dependence suggests that simple few-particle models based on the dense-fluid, cell-model picture will not be particularly useful for thermal conductivity. This is a little surprising in view of the great success of an Einstein-like model for conductivity in generating a good corresponding-states account of conductivities for a wide range of force laws over the entire span of dense-fluid conditions.<sup>(18)</sup>

The uncertainty in the old Green-Kubo results was 2% after 2 million collisions per particle ( $V/V_0 = 1.80$ ,  $N = 108$ ). Our uncertainty of extrapolated  $\kappa_E$  (based on 200,000 collisions in total) is 3% for  $N = 32$ . This is only a relatively small improvement over the estimate based on statistical fluctuations proportional to the square root of the number of collisions studied. The relatively complicated dependence of the results on field strength suggests that the external field method is advantageous only if it is desired to know the nonlinear conductivity. The linear conductivity can as easily be found using the Green-Kubo technique, which has the added advantage of providing the other transport coefficients and their frequency dependence simultaneously.

The nonlinear conductivity is interesting. Both the four-sphere and 32-sphere results are approximately linear in  $\lambda^{1/2}$  for larger fields. This dependence can be thought of as arising from a diffusion process or from a scattering process. In the former case the diffusion equation suggests a falloff in correlation as time<sup>3/2</sup> in three dimensions, leading to a frequency dependence or field dependence of order  $\omega^{1/2}$  or  $\lambda^{1/2}$ . Alternatively, from the standpoint of scattering of phonons, the Debye-Waller scattering, proportional to the average value of  $\omega^{-2}$ , and combined with a density of states proportional to  $\omega^2$  leads also to a square-root dependence.

The nonlinear conductivities found here, increasing with field in the solid and dense fluid phases, could be extended and made more precise were there data available from other simulations for comparison. There appear to be no difficulties in extending the nonequilibrium techniques to hard spheres. The hard-sphere model is also suited to shock wave simulation, the area in which nonlinear effects are most easily generated and studied.

## APPENDIX A. ISOKINETIC HARD-SPHERE COLLISIONS

The colliding motion begins at time 0 and ends at time  $t_e$  with  $r_{12} \equiv \sigma$  in both cases. We assume that the force during the penetration of the spheres is

$$\mathbf{F}_{12} = F \hat{\mathbf{e}}_{12} \quad (\text{A1})$$

where  $F$  is an arbitrarily high, but finite, constant. Then, (24), (25), and (27) may be combined to give a single differential equation for  $\zeta_K$ :

$$\begin{aligned} \dot{\zeta}_K &= F^2 [(1 + \frac{1}{2}\delta)/mK] - \zeta_K^2 \\ \delta &\equiv \frac{1}{2}(1 - 2N^{-1}) \lambda^2 x_{12}^2 \geq 0 \end{aligned} \quad (\text{A2})$$

For the duration of each collision  $\delta$  is fixed, and gives the influence of the driving force  $F_i^d$  on the collision. It is convenient to replace the time variables  $\zeta$  and  $t$  by impulse variables  $X_K$  and  $\tau$ :

$$X_K \equiv \zeta_K/F, \quad \tau \equiv Ft \quad (\text{A3})$$

During the collision,  $0 < \tau < \tau_e$ . In the hard-sphere limit, as the collision time  $t_e$  tends to zero, the absolute value of  $\zeta_K$  becomes arbitrarily large, but  $\tau_e$  and  $\zeta_K$  remain nonvanishing and finite, respectively. We will see that similar considerations hold for pressure and heat flux. Using the definitions (A3), we find that Eq. (A2) becomes

$$\begin{aligned} dX_K/d\tau &= (d\zeta_K/dt)/F^2 = q^2 - X_K^2 \\ q &\equiv [(1 + \frac{1}{2}\delta)/mK]^{1/2} \end{aligned} \quad (\text{A4})$$

From the definition of  $q$  and  $X_K$  it follows that

$$-q \leq \hat{X}_K < q \quad (\text{A5})$$

with  $\hat{X}_K \equiv X_K(t=0)$ . If  $\hat{X}_K > -q$ , the solution of (A4) is

$$\begin{aligned} X_K &= q[1 - 2/(1 + \Omega \exp 2q\tau)] \\ \Omega &\equiv (q + \hat{X}_K)/(q - \hat{X}_K), \quad 0 < \Omega < \infty \end{aligned} \quad (\text{A6})$$

$X_K$  increases monotonically with time. Because we know the friction, Eqs. (17) can be solved separately; see (19). The result is

$$\mathbf{p}_i(\tau) = [I(\tau)]^{-1} \left[ \hat{p}_i + \hat{e}_{12} N_i \int_0^\tau I(\tau') d\tau' \right]$$

$$I(\tau) = [\Omega \exp(q\tau) + \exp(-q\tau)] / (1 + \Omega) \quad (\text{A7})$$

$$\int_0^\tau I(\tau') d\tau' = [1 - \Omega + \Omega \exp(q\tau) - \exp(-q\tau)] / [q(1 + \Omega)]$$

Now it has to be determined when the collision ends. The condition corresponding to  $r'_{12}(\tau_e) = r_{12}(\tau_e) = \sigma$  is

$$\int_0^{\tau_e} p'_{12}(\tau) d\tau = Fm[r'_{12}(\tau_e) - \sigma] = 0 \quad (\text{A8})$$

From (A7), this can be written as

$$\ln I(\tau_e) = -d_a \tan^{-1} d_b(\tau_e) \quad (\text{A9})$$

$$d_a \equiv [1 - \Omega + \frac{1}{2}(1 + \Omega) q \hat{p}'_{12}] / \Omega^{1/2}$$

$$d_b(\tau_e) \equiv \Omega^{1/2} [\exp(q\tau_e) - 1] / [1 + \Omega \exp(q\tau_e)]$$

As usual,  $\hat{p}'_{12} \equiv p'_{12}(\tau=0)$ . The trivial solution of (A9) with  $\tau=0$  corresponds to the *beginning* of the collision. There is a second unique solution with  $0 < \tau_e < \infty$  determining the *end* of the collision. This solution has to be found numerically. Then, the pressure (28) and heat flux (29) integrals yield

$$\int_{\text{coll}} P_{\alpha\beta} V dt = s \hat{e}_{\alpha,12} \hat{e}_{\beta,12} t_c \quad (\text{A10})$$

$$\int_{\text{coll}} mQ_x V dt = \frac{1}{2} s \hat{e}_{\alpha,12} \int_{\text{coll}} s'_{12}(t) dt$$

$$= \frac{1}{2} s \hat{e}_{\alpha,12} [(1 + L) / (qL^{1/2})]$$

$$\times [s'_{12} - \frac{1}{2} g \hat{x}_{12} (1 - 2N^{-1}) \hat{p}'_{12}] \tan^{-1} d_b(t_c) \quad (\text{A11})$$

For  $d_b(\tau_e)$ , see (A9). Combination of (27), (29), and (A8) results in

$$\int_{\text{coll}} \zeta_K dt = \int_{\text{coll}} X_K d\tau = [\lambda / (2Km)] \int_{\text{coll}} mQ_x V dt \quad (\text{A12})$$

Thus, the complete solution for  $\hat{X}_K > -q$  has been found. If  $\hat{X}_K$  is equal to  $-q$ , a limiting case of zero probability,  $\tau_e$  diverges. The isokinetic case is not well-posed then.

## APPENDIX B. ISOENERGETIC HARD-SPHERE COLLISIONS

The three coupled equations for the isoenergetic case are

$$\dot{p}'_{12} = F_{12}[2 - \lambda \hat{x}_{12} s'_{12} p'_{12} / (4Km)] \quad (\text{B1})$$

$$\dot{s}'_{12} = F_{12} \lambda \hat{x}_{12} [(1 - 2N^{-1}) - ((s'_{12})^2 / (4Km))] \quad (\text{B2})$$

$$\dot{K}m = F_{12} p'_{12} \quad (\text{B3})$$

The corresponding expressions for  $\zeta_E$ ,  $P_{\alpha\beta}$ , and  $Q_\alpha$  are given by (26), (28), and (29), respectively.

Away from equilibrium ( $\lambda \neq 0$ ) and for  $N > 2$ , the case  $\delta = 0$  has vanishing probability. Compare (A2). The same is true if  $K$  becomes zero at the turning point. The solution of both these cases can be found using the assumption that  $F_{12}$  is constant. However, we will not give the results of these special cases, and turn now to the general case  $\delta > 0$ ,  $K > 0$ .

We introduce the new variables  $u$ ,  $v$ ,  $w$ ,

$$u \equiv \frac{1}{2} \lambda \hat{x}_{12} s'_{12}, \quad v \equiv \frac{1}{2} \delta p'_{12}, \quad w = 2\delta Km \quad (\text{B4})$$

into (B1)–(B3) and find

$$\dot{u} = \delta F_{12} [1 - (u^2/w)] \quad (\text{B5})$$

$$\dot{v} = \delta F_{12} [1 - (uv/w)] \quad (\text{B6})$$

$$\dot{w} = \delta F_{12} [4v/\delta] \quad (\text{B7})$$

$F_{12} \gg 0$  is not yet specified. In the above variables,

$$\zeta_E = \delta F_{12} u/w \quad (\text{B8})$$

See (26).

Assuming that  $F_{12}$  is constant is not useful here, but a more complicated assumption *does* make the system tractable:

$$F_{12} = Cw \operatorname{sgn}(u) / (u\delta) \quad (\text{B9})$$

Thus,  $F_{12}$  varies during the collision.  $C$  is an arbitrary, large, positive constant. Because in the general case of  $\delta > 0$  and  $w > 0$ ,  $F_{12} \gg 0$ . Thus,  $C \rightarrow \infty$  yields again the hard-sphere limit. If  $u$  changes sign during the collision,  $F_{12}$  would approach  $\infty$  at this point even for finite  $C$ . We will see later that this causes no difficulty. The friction coefficient becomes

$$\zeta_E = C \operatorname{sgn}(u) \quad (\text{B10})$$

Defining  $\tau \equiv Ct$ , (B5)–(B7) become

$$du/d\tau = \text{sgn}(u) [w - u^2]/u \quad (\text{B11})$$

$$dv/d\tau = \text{sgn}(u) [w - uv]/u \quad (\text{B12})$$

$$dw/d\tau = \text{sgn}(u) [4wv]/(\delta u) \quad (\text{B13})$$

Subtracting (B11) from (B12) yields

$$d(v - u)/d\tau = -\text{sgn}(u) [v - u] \quad (\text{B14})$$

This can be solved, with the result:

$$\begin{aligned} v(\tau) - u(\tau) &= (\hat{v} - \hat{u}) \text{ex}(\tau) \\ &\quad \exp(-\tau), \quad \hat{u} \geq 0 \\ \text{ex}(\tau) \equiv &\quad \exp(\tau), \quad 0 \geq u \\ &\quad \exp(2\tau^* - \tau), \quad u > 0 > \hat{u} \end{aligned} \quad (\text{B15})$$

From the definitions of  $u$  and  $w$  it follows that  $w > u^2$ . Therefore,  $du/d\tau > 0$  during the collision; see (B11). Thus,  $u > \hat{u}$  for  $\tau > 0$ . The quantity  $\tau^*$  is defined by  $u(\tau^*) = 0$ , i.e., when  $u$  changes sign (which need not happen). Since  $\text{ex}(\tau)$  determines the time behavior of  $(v - u)$ , we define a function  $g(\tau)$  via

$$u(\tau) \equiv g(\tau) \text{ex}(\tau) \quad (\text{B16})$$

It follows that

$$\hat{g} = \hat{u}, \quad \text{sgn}(g) = \text{sgn}(u), \quad du/d\tau = [dg/d\tau - \text{sgn}(g) g] \text{ex}(\tau) \quad (\text{B17})$$

Inserting (B15) yields

$$v = (g + \hat{v} - \hat{u}) \text{ex}(\tau) \quad (\text{B18})$$

On the other hand, from (B11) and (B17) it follows that

$$w = \text{sgn}(g) g(dg/d\tau) \text{ex}^2(\tau) \quad (\text{B19})$$

Thus, we have expressed  $u$ ,  $v$ , and  $w$  in terms of a single unknown function  $g$ . Here  $(du/d\tau) > 0$  means  $(dg/d\tau) > 0$ ; see (B17). Thus,  $g$  is strictly increasing with  $\tau$ . The relation  $g(\tau^*) = 0$  defines  $\tau^*$ . Generally,  $w$  is nonnegative, due to (B19). Because  $w$  is proportional to  $K > 0$ ,  $w$  cannot vanish, even for  $g \rightarrow 0$ . This means that at  $\tau \rightarrow \tau^*$ ,  $|g| (dg/d\tau)$  remains finite and nonzero. That  $(dg/d\tau) \rightarrow \infty$  when  $\tau \rightarrow \tau^*$  we can also see from (B11).

Utilizing (B13) yields the desired differential equation for  $g$ :

$$[g(d^2g/d\tau^2) - (dg/d\tau)^2] \delta \text{sgn}(g) = 2(dg/d\tau)[g(\delta + 2)g + 2(\hat{v} - \hat{u})] \quad (\text{B20})$$

Using the transformation  $p \equiv dg/d\tau$ , one can solve the resulting first-order differential equation in  $p$  (as function of  $g$ ). Reinserting  $p = dg/d\tau$  yields

$$\begin{aligned} g dg/(ag^2 + bg + c) &= \text{sgn}(g) d\tau \\ a &\equiv 1 + 2/\delta, \quad b \equiv (4/\delta)(\hat{v} - \hat{u}), \quad c \equiv \hat{w} - a\hat{u}^2 - b\hat{u} \end{aligned} \quad (\text{B21})$$

The denominator is nonvanishing for any  $g$  if

$$\Delta \equiv 4ac - b^2 = 4[1 + (2/\delta)] \hat{w} - 4[\hat{u} + (2/\delta) \hat{v}]^2 > 0 \quad (\text{B22})$$

From the definition of  $u$ ,  $v$ , and  $w$  it follows that  $\Delta$  is positive if  $\delta > 0$ . Equation (B21) can be solved for  $\tau$  as a function of  $g$ :

$$\text{ex}(\tau) = \left[ \frac{a\hat{g}^2 + b\hat{g} + c}{ag^2 + bg + c} \right]^{1/(2a)} \exp \left( \frac{b}{a\Delta^{1/2}} \tan^{-1} \frac{\Delta^{1/2}(g - \hat{g})}{2a(g\hat{g}) + b(g + \hat{g}) + 2c} \right) \quad (\text{B23})$$

Combining (B19) and (B21) yields the simple relations

$$w = (ag^2 + bg + c) \text{ex}^2(\tau), \quad \hat{w} = a\hat{g}^2 + b\hat{g} + c \quad (\text{B24})$$

The end of the collision is given by the condition that the kinetic energy is the same as at the same as at the beginning of the collision, i.e.,  $w_e = \hat{w}$ . Thus,

$$\text{ex}(\tau_e) = [\hat{w}/(ag_e^2 + bg_e + c)]^{1/2} \quad (\text{B25})$$

Inserting this result in (B23) yields an equation for  $g_e$ :

$$(1 - a) \Delta^{1/2} \ln \frac{ag_e^2 + bg_e + c}{\hat{w}} = 2b \tan^{-1} \frac{\Delta^{1/2}(g_e - \hat{g})}{2ag_e\hat{g} + b(g_e + \hat{g}) + 2c} \quad (\text{B26})$$

This equation has a unique solution for  $g_e > \hat{g}$ , which has to be determined numerically. This may be compared with the general isokinetic case, where a formally similar but simpler equation, (A9), gave  $\tau_e$ .

We may evaluate  $\tau_e$  using (B25) and the solution of (B26). It is possible, however, to express all quantities in terms of  $g_e$ . For  $u$ ,  $v$ ,  $w$ , see Eqs. (B16), (B18), and (B24), respectively, inserting (B25) for  $\text{ex}(\tau)$ . Bearing in mind that  $\zeta_E = C \text{sgn}(u)$ , Eq. (B10), we obtain for the momenta at the end of collision

$$\mathbf{p}_i(g_e) = \text{ex}[\tau(g_e)] [\hat{\mathbf{p}}_i + \hat{\mathbf{e}}_{12} N_i (g_e - \hat{g})/\delta] \quad (\text{B27})$$

[cf. (19)]. Furthermore, the collisional integral of the friction coefficient is given by

$$\int_{\text{coll}} \zeta_E dt = -\ln \text{ex}(\tau_e) = \frac{1}{2} \ln [(ag_e^2 + bg_e + c)/\hat{w}] \quad (\text{B28})$$

The corresponding pressure and heat flux contributions are evaluated easily numerically:

$$\int_{\text{coll}} P_{\alpha\beta} V dt = \sigma \hat{e}_{\alpha,12} \hat{e}_{\beta,12} \delta^{-1} \int_{\hat{g}}^{g_e} \text{ex}[\tau(g)] dg \quad (\text{B29})$$

$$\int_{\text{coll}} m Q_{\alpha} V dt = \sigma \hat{e}_{\alpha,12} (\delta \lambda \hat{\chi}_{12})^{-1} \int_{\hat{g}}^{g_e} \text{ex}^2[\tau(g)] g dg \quad (\text{B30})$$

which completes the solution of the general case.

## APPENDIX C

The results of the computer experiments are gathered in Tables III-VIII.

Table III. Results of Nonequilibrium Molecular Dynamics for Hard Spheres:  
 $N=4$ ,  $V/V_0=1.25^a$

$\lambda^{1/2}$	$10^2 \bar{\Gamma}^{\text{str}}$	$Z_E$	$\bar{Q}_{x,E}$	$\kappa_E/k$	$\kappa^{\text{str}}/k$	$(Z_K-1)/(Z_E-1)$	$\kappa_K^{\text{coll}}/\kappa_E^{\text{coll}}$
0.0	1.242(3)	14.36(0)	—	—	—	1.126	—
0.1	1.242(2)	14.36(0)	—	—	—	1.124	—
0.2	1.243(3)	14.36(0)	0.17(6)	4.29(144)	0.24(15)	1.126	1.379
0.3	1.243(3)	14.36(0)	0.60(7)	6.65(79)	0.56(8)	1.125	1.461
0.4	1.244(2)	14.37(0)	0.77(9)	4.80(58)	0.38(5)	1.125	1.484
0.5	1.242(4)	14.37(0)	1.25(7)	5.01(28)	0.38(2)	1.126	1.408
0.6	1.242(4)	14.37(1)	1.89(8)	5.25(23)	0.38(2)	1.124	1.396
0.7	1.236(3)	14.39(1)	2.81(11)	5.73(23)	0.43(1)	1.121	1.398
0.8	1.233(4)	14.40(1)	3.28(16)	5.13(25)	0.38(2)	1.122	1.406
0.9	1.234(6)	14.40(2)	4.14(14)	5.12(17)	0.37(1)	1.120	1.392
1.0	1.228(3)	14.41(2)	5.10(14)	5.10(14)	0.37(1)	1.117	1.375
1.1	1.229(4)	14.45(1)	5.71(10)	4.72(12)	0.33(1)	1.117	1.363
1.2	1.221(5)	14.43(2)	6.67(21)	4.63(14)	0.32(1)	1.115	1.356
1.3	1.217(2)	14.39(2)	7.38(7)	4.37(4)	0.29(1)	1.112	1.344
1.4	1.231(5)	14.32(2)	8.32(13)	4.25(7)	0.27(1)	1.112	1.334
1.5	1.226(5)	14.29(4)	8.73(13)	3.88(6)	0.24(1)	1.110	1.321
1.6	1.245(5)	14.18(2)	9.53(7)	3.72(3)	0.22(0)	1.110	1.319
1.7	1.243(7)	14.13(3)	10.16(14)	3.52(5)	0.20(0)	1.107	1.307
1.8	1.263(6)	13.88(3)	10.53(8)	3.25(2)	0.18(0)	1.105	1.295
1.9	1.265(4)	13.81(4)	10.87(9)	3.01(2)	0.15(0)	1.103	1.280
2.0	1.287(3)	13.66(4)	11.30(6)	2.83(1)	0.14(0)	1.103	1.274

<sup>a</sup>The calculated quantities are explained in Table II. Numbers in parentheses denote the uncertainty of the last digit(s).

Table IV. As Table III, Except for  $N=32$ ,  $V/V_0=1.25$

$\lambda^{1/2}$	$10^2 \bar{r}^{\text{str}}$	$Z_E$	$\bar{Q}_{N,E}$	$\kappa_E/k$	$\kappa^{\text{str}}/k$	$(Z_K-1)/(Z_E-1)$	$\kappa_K^{\text{coll}}/\kappa_E^{\text{coll}}$
0.0	0.137(0)	14.67(1)	—	—	—	1.011	—
0.1	0.137(0)	14.68(1)	—	—	—	1.011	—
0.2	0.137(0)	14.67(1)	0.9(1)	21.5(32)	1.34(25)	1.011	1.033
0.3	0.137(0)	14.68(1)	1.6(1)	17.6(15)	1.11(12)	1.011	1.034
0.4	0.138(1)	14.65(1)	2.7(1)	17.0(7)	1.10(5)	1.011	1.035
0.5	0.137(0)	14.66(1)	4.0(2)	15.9(7)	1.04(5)	1.011	1.037
0.6	0.138(1)	14.63(1)	6.1(2)	16.8(6)	1.10(4)	1.011	1.039
0.7	0.139(1)	14.56(2)	8.4(3)	17.2(5)	1.15(5)	1.012	1.041
0.8	0.139(1)	14.56(3)	10.5(3)	16.5(5)	1.11(4)	1.012	1.040
0.9	0.141(1)	14.51(3)	14.3(5)	17.6(7)	1.14(15)	1.013	1.048
1.0	0.142(1)	14.44(5)	18.2(5)	18.2(5)	1.32(5)	1.014	1.054
1.1	0.144(1)	14.47(5)	23.3(5)	19.2(4)	1.43(4)	1.015	1.059
1.2	0.149(1)	14.31(5)	28.2(6)	19.6(4)	1.51(4)	1.017	1.066
1.3	0.155(1)	14.13(7)	33.3(7)	19.7(4)	1.57(5)	1.019	1.077
1.4	0.165(1)	13.74(7)	38.7(11)	19.7(6)	1.63(7)	1.022	1.086
1.5	0.174(1)	13.53(4)	43.1(7)	19.2(3)	1.61(3)	1.024	1.091
1.6	0.182(2)	13.25(10)	46.0(10)	18.0(4)	1.54(3)	1.025	1.091
1.7	0.204(1)	12.79(8)	53.3(9)	18.4(3)	1.59(2)	1.030	1.103
1.8	0.212(3)	12.41(10)	54.0(9)	16.7(3)	1.47(3)	1.030	1.101
1.9	0.230(3)	12.13(7)	58.7(7)	16.3(2)	1.46(1)	1.032	1.105
2.0	0.256(3)	11.72(6)	62.3(6)	15.6(2)	1.42(1)	1.035	1.109

Table V. As Table III, Except for  $N=4$ ,  $V/V_0=1.80$

$\lambda^{1/2}$	$10^2 \bar{r}^{\text{str}}$	$Z_E$	$\bar{Q}_{N,E}$	$\kappa_E/k$	$\kappa^{\text{str}}/k$	$(Z_K-1)/(Z_E-1)$	$\kappa_K^{\text{coll}}/\kappa_E^{\text{coll}}$
0.0	3.12(1)	6.30(1)	—	—	—	1.125	—
0.1	3.12(1)	6.32(1)	—	—	—	1.124	—
0.2	3.13(1)	6.31(1)	0.06(2)	1.53(48)	0.32(8)	1.125	1.480
0.3	3.12(1)	6.31(1)	0.19(2)	2.15(25)	0.34(4)	1.124	1.398
0.4	3.13(1)	6.32(1)	0.36(3)	2.26(19)	0.37(3)	1.126	1.432
0.5	3.13(2)	6.31(1)	0.62(3)	2.48(11)	0.41(2)	1.123	1.409
0.6	3.13(2)	6.31(1)	0.80(4)	2.22(10)	0.34(2)	1.126	1.388
0.7	3.11(1)	6.33(1)	1.10(5)	2.24(9)	0.36(1)	1.124	1.391
0.8	3.10(1)	6.34(2)	1.32(4)	2.06(6)	0.32(1)	1.122	1.379
0.9	3.12(1)	6.34(1)	1.65(5)	2.03(6)	0.32(1)	1.123	1.384
1.0	3.11(1)	6.36(2)	1.92(3)	1.92(3)	0.30(1)	1.121	1.375
1.1	3.12(2)	6.36(3)	2.33(4)	1.93(3)	0.30(1)	1.122	1.379
1.2	3.13(2)	6.34(2)	2.63(2)	1.83(1)	0.28(0)	1.121	1.369
1.3	3.14(2)	6.35(1)	2.98(4)	1.76(2)	0.27(0)	1.122	1.370
1.4	3.19(1)	6.29(2)	3.22(3)	1.64(2)	0.25(0)	1.121	1.358
1.5	3.16(2)	6.35(3)	3.57(5)	1.59(2)	0.23(0)	1.123	1.360
1.6	3.21(2)	6.28(5)	3.76(5)	1.47(2)	0.21(0)	1.124	1.355
1.7	3.27(2)	6.20(4)	3.98(5)	1.38(2)	0.20(0)	1.125	1.354
1.8	3.32(2)	6.18(4)	4.25(4)	1.31(1)	0.19(0)	1.129	1.356
1.9	3.36(2)	6.18(4)	4.38(3)	1.21(1)	0.17(0)	1.132	1.358
2.0	3.32(3)	6.31(6)	4.77(7)	1.19(2)	0.16(0)	1.138	1.369

Table VI. As Table III, Except for  $N=32$ ,  $V/V_0=1.80$

$\lambda^{1/2}$	$10^2 i^{\text{str}}$	$Z_E$	$\bar{Q}_{x,E}$	$\kappa_E/k$	$\kappa^{\text{str}}/k$	$(Z_K-1)/(Z_E-1)$	$\kappa_K^{\text{coll}}/\kappa_E^{\text{coll}}$
0.0	0.285(1)	7.58(2)	--	--	--	1.011	--
0.1	0.284(1)	7.57(3)	--	--	--	1.011	--
0.2	0.282(1)	7.62(3)	0.3(1)	7.3(13)	0.83(21)	1.011	1.039
0.3	0.282(1)	7.62(3)	0.6(0)	6.2(3)	0.84(6)	1.011	1.038
0.4	0.285(1)	7.58(3)	1.1(1)	7.0(4)	0.89(7)	1.011	1.038
0.5	0.283(2)	7.62(5)	1.7(1)	6.8(3)	0.78(8)	1.011	1.037
0.6	0.285(2)	7.64(3)	2.6(1)	7.3(3)	0.87(5)	1.012	1.043
0.7	0.288(3)	7.59(6)	3.6(2)	7.4(4)	0.89(3)	1.012	1.042
0.8	0.294(2)	7.50(5)	5.3(2)	8.3(4)	1.10(6)	1.013	1.055
0.9	0.308(2)	7.29(6)	6.7(3)	8.3(4)	1.22(7)	1.014	1.062
1.0	0.332(3)	7.13(5)	9.8(3)	9.8(3)	1.48(5)	1.019	1.078
1.1	0.354(2)	7.05(7)	12.9(4)	10.7(3)	1.64(4)	1.022	1.087
1.2	0.382(6)	6.86(7)	15.1(5)	10.5(3)	1.73(10)	1.027	1.104
1.3	0.428(4)	6.68(5)	18.5(6)	10.9(4)	1.83(5)	1.032	1.118
1.4	0.458(6)	6.54(7)	20.2(3)	10.3(2)	1.77(5)	1.035	1.121
1.5	0.520(8)	6.37(8)	23.6(5)	10.5(2)	1.81(3)	1.041	1.136
1.6	0.565(7)	6.21(8)	24.5(5)	9.6(2)	1.73(4)	1.044	1.135
1.7	0.611(7)	5.99(6)	25.6(4)	8.9(1)	1.62(1)	1.045	1.134
1.8	0.677(7)	5.80(8)	26.9(5)	8.3(2)	1.56(2)	1.049	1.141
1.9	0.710(11)	5.70(6)	27.4(5)	7.6(1)	1.44(2)	1.049	1.137
2.0	0.734(12)	5.73(9)	29.2(3)	7.3(1)	1.37(2)	1.050	1.136

Table VII. As Table III, Except for  $N=4$ ,  $V/V_0=3.00$

$\lambda^{1/2}$	$10^2 i^{\text{str}}$	$Z_E$	$\bar{Q}_{x,E}$	$\kappa_E/k$	$\kappa^{\text{str}}/k$	$(Z_K-1)/(Z_E-1)$	$\kappa_K^{\text{coll}}/\kappa_E^{\text{coll}}$
0.0	5.88(3)	3.82(1)	--	--	--	1.125	--
0.1	5.91(3)	3.80(2)	--	--	--	1.124	--
0.2	5.86(3)	3.83(1)	0.05(1)	1.33(28)	0.29(7)	1.125	1.378
0.3	5.87(3)	3.82(2)	0.11(1)	1.26(14)	0.27(4)	1.126	1.355
0.4	5.92(3)	3.81(2)	0.19(1)	1.21(6)	0.29(3)	1.125	1.398
0.5	5.88(3)	3.83(2)	0.30(1)	1.20(5)	0.30(2)	1.124	1.366
0.6	5.85(6)	3.82(3)	0.42(1)	1.15(4)	0.28(1)	1.123	1.362
0.7	5.91(6)	3.82(3)	0.56(2)	1.13(4)	0.28(1)	1.125	1.374
0.8	6.10(4)	3.73(2)	0.70(3)	1.10(4)	0.29(1)	1.122	1.342
0.9	6.08(5)	3.76(2)	0.81(2)	1.00(2)	0.26(1)	1.125	1.359
1.0	6.09(3)	3.74(1)	0.91(2)	0.91(2)	0.23(0)	1.124	1.340
1.1	6.19(6)	3.71(2)	1.06(2)	0.87(1)	0.22(1)	1.122	1.327
1.2	6.24(3)	3.69(2)	1.16(1)	0.80(1)	0.22(1)	1.123	1.330
1.3	6.33(4)	3.65(2)	1.28(1)	0.76(1)	0.21(0)	1.124	1.334
1.4	6.61(4)	3.53(2)	1.33(2)	0.68(1)	0.20(0)	1.122	1.334
1.5	6.69(3)	3.52(2)	1.40(1)	0.62(1)	0.19(0)	1.123	1.330
1.6	6.94(3)	3.42(2)	1.47(2)	0.58(1)	0.18(0)	1.121	1.325
1.7	6.78(22)	3.38(2)	1.55(2)	0.54(1)	0.17(0)	1.120	1.311
1.8	7.27(6)	3.32(2)	1.61(2)	0.50(1)	0.16(0)	1.113	1.308
1.9	7.47(4)	3.23(2)	1.63(2)	0.45(1)	0.15(0)	1.115	1.296
2.0	7.71(11)	3.17(4)	1.67(2)	0.42(1)	0.15(0)	1.116	1.295

Table VIII. The Results of Tables III–VII Extrapolated to Equilibrium<sup>a</sup>

$N$	$V/V_0$	$10^2 \hat{P}^{\text{str}*}$	$Z_E^*$	$\kappa_E^*/k$	$\kappa^{\text{str}*}/k$
4	1.25	1.243(0)	14.362(2)	5.18(18)	0.39(2)
32	1.25	0.137(0)	14.666(5)	16.74(36)	1.09(2)
4	1.80	3.124(2)	6.312(2)	2.30(8)	0.37(2)
32	1.80	0.284(1)	7.603(10)	6.79(21)	0.85(2)
4	3.00	5.885(9)	3.820(5)	1.18(2)	0.28(0)

<sup>a</sup> Indicated by an asterisk. Numbers in parentheses denote the uncertainty of the last digit(s).

## APPENDIX D

In this Appendix, we derive Eq. (33). Since  $Z^{\text{str}} = P^{\text{str}}V/NkT = 1$  for hard spheres (see Section 3.1) Eq. (33) can be written as

$$P_E^{\text{coll}}V/P_K^{\text{coll}}V = 1 - D(N-1), \quad D(N-1) \geq 1 \quad (\text{D1})$$

valid for vanishing driving force,  $\lambda = 0$ . In both isoenergetic and isokinetic cases,  $P^{\text{coll}}V$  may be evaluated as a time average,

$$P^{\text{coll}}V = (sD)^{-1} \sum_{\text{coll}} \int_{\text{coll}} \left[ \sum_{\alpha} P_{\alpha\alpha}(t) \right] V dt \quad (\text{D2})$$

Compare with Eq. (11). The first sum goes over all collisions observed during the large time interval  $s$ . According to (28), the integrand may be written as

$$\sum_{\alpha} P_{\alpha\alpha}(t) V = F_{12} \sigma \quad (\text{D3})$$

$F_{12} = F$  is assumed to be constant. See (A1) for the isokinetic case. The same assumption applies in the isoenergetic case if  $\lambda = 0$ . This special case was not treated in Appendix B. Then it follows that

$$\int_{\text{coll}} \sum_{\alpha} P_{\alpha\alpha}(t) V dt = \sigma \tau_e \quad (\text{D4})$$

for both isoenergetic and isokinetic cases, where  $\tau_e$  is defined in parallel to Eq. (A3). Since  $\lambda = 0$ ,  $\tau_e$  can be calculated analytically; the result is

$$\tau_{e,E} = -\hat{P}'_{12} \quad (\text{D5})$$

$$\tau_{e,K} = (mK)^{1/2} \ln \{ [(4mK)^{1/2} - \hat{p}'_{12}] / [(4mK)^{1/2} + \hat{p}'_{12}] \} \quad (\text{D6})$$

$\tau_{e,K}$  comes from Eq. (A9),  $\lambda=0$  inducing

$$(d_a=0) \rightarrow I(\tau_e) = 1 \quad (\text{D7})$$

Combining Eqs. (D4)–(D6) yields the integral occurring in (D2) for both isoenergetic and isokinetic cases.

For calculating  $P_E^{\text{coll}}V$  and  $P_K^{\text{coll}}V$  we use the ensemble average instead of the time average. The probability of a collision is proportional to  $(-\hat{p}'_{12}) > 0$ . Furthermore, the system is isotropic for  $\lambda=0$ . The momenta are restricted by the fixed center of mass and the fixed streaming kinetic energy  $K^{\text{str}}$ ,

$$\sum_i \hat{p}_{\alpha i} = 0, \quad \alpha = x, y, \dots \quad (\text{D8})$$

$$\sum_{\alpha} \sum_i \hat{p}_{\alpha i}^2 = 2mK^{\text{str}}, \quad 1 \leq i \leq N. \quad (\text{D9})$$

Inserting (D8) into (D9) yields

$$\sum_{\alpha} \sum_i \hat{p}_{\alpha i}^2 + \sum_{\alpha} \left( \sum_i \hat{p}_{\alpha i} \right)^2 = 2mK^{\text{str}}, \quad 1 \leq i \leq N-1 \quad (\text{D10})$$

Thus, we have  $(N-1)D$  variables  $\hat{p}_{\alpha i}$  in momentum space with one restriction forcing the points to lie on an ellipsoid. Transformation to  $(N-1)D$  variables  $w_j$  is always possible so that the allowed points lie on the surface of a unit hypersphere:

$$\sum_j w_j^2 = 1, \quad 1 \leq j \leq (N-1)D \quad (\text{D11})$$

$$0 < w_1 = (-\hat{p}'_{12}) / (4mK^{\text{str}})^{1/2} \leq 1 \quad (\text{D12})$$

Thus, the probability of a collision is proportional to  $w_1$ . The ensemble average of a function  $f(w_1)$  becomes

$$f = \frac{\int_0^1 f(w_1) w_1 dw_1 \int \dots \int dw_2 \dots dw_{(N-1)D}}{\int_0^1 w_1 dw_1 \int \dots \int dw_2 \dots dw_{(N-1)D}}, \quad (N-1)D \geq 2 \quad (\text{D13})$$

with the restriction (C12). Carrying out the integrals over  $w_2 \dots w_{(N-1)D}$  and replacing  $w_1$  by  $w$  gives

$$\langle f \rangle = \frac{\int_0^1 f(w) w(1-w^2)^{[(N-1)D-3]/2} dw}{\int_0^1 w(1-w^2)^{[(N-1)D-3]/2} dw} \quad (\text{D14})$$

In order to obtain (D1), we have to specify  $f(w)$ :

$$P_E^{\text{coll}} V / P_K^{\text{coll}} V = \langle \tau_{e,E}(w) \rangle / \langle \tau_{e,K}(w) \rangle \quad (\text{D15})$$

$$\tau_{e,E} = 2(mK^{\text{str}})^{1/2} w$$

$$\tau_{e,K} = (mK)^{1/2} \ln[(1+w)/(1-w)] \quad (\text{D16})$$

$K^{\text{str}}$ , the isoenergetic streaming energy, is equal to the isokinetic  $K$ . It follows that

$$\frac{P_E^{\text{coll}} V}{P_K^{\text{coll}} V} = \frac{\int_0^1 dw w^2 (1-w^2)^{[(N-1)D-3]/2}}{\int_0^1 dw w (1-w^2)^{(N-1)D-3} \ln[(1+w)/(1-w)]} \quad (\text{D17})$$

Evaluation of this ratio yields (D1) for  $(N-1)D \geq 2$ . If  $N=2$  and  $D=1$ ,  $j=1$  and  $w_1=1$  are fixed [see (D11), (D12)]. Thus, no average has to be taken in (D15). Due to  $w=w_1=1$ , the numerator is finite, the denominator infinite, in accordance with (D1) for the case  $(n-1)D=1$ .

## ACKNOWLEDGMENTS

W. G. H. thanks the Universities of California and Vienna, as well as the Lawrence Livermore National Laboratory, for support during a sabbatical leave which led to this work. Work at the Lawrence Livermore National Laboratory was carried out under contract W-7405-ENG-48. Work at the University of Vienna was carried out with the active encouragement of Prof. Peter Weinzierl. Mag. Karlsreiter provided invaluable help with the computer system at the University of Vienna. Dr. Stanislaw Kaluza calculated the data exhibited in Tables III-VII from the computer results.

## REFERENCES

1. S. Chapman and T. G. Cowling, *The Mathematical Theory of Non-Uniform Gases* (Cambridge University Press, 1970).
2. B. J. Alder and T. E. Wainwright, *J. Chem. Phys.* **33**:1439 (1960).
3. B. J. Alder, D. M. Gass, and T. E. Wainwright, *J. Chem. Phys.* **53**:3813 (1970).
4. W. G. Hoover and B. J. Alder, *J. Chem. Phys.* **46**:686 (1967).
5. W. G. Hoover and F. H. Ree, *J. Chem. Phys.* **49**:3609 (1968).
6. H. S. Kang, C. S. Lee, T. Ree, and F. H. Ree, *J. Chem. Phys.* **84**:4547 (1986).
7. W. G. Hoover, *Phys. Today* **37**:44 (1984).
8. D. J. Evans and W. G. Hoover, *Annu. Rev. Fluid Mech.* **10**:243 (1986).
9. D. J. Evans, *Phys. Lett.* **91A**:457 (1982).
10. M. Dixon and M. J. Gillan, *J. Phys. C* **16**:869 (1983).

11. W. G. Hoover, B. Moran, and J. Haile, *J. Stat. Phys.* **37**:109 (1983).
12. W. G. Hoover, G. Ciccotti, G. Paolini, and C. Massobrio, *Phys. Rev. A* **32**:3765 (1986).
13. W. G. Hoover and K. W. Kratky, *J. Stat. Phys.* **42**:1103 (1986).
14. W. G. Hoover, *J. Stat. Phys.* **42**:587 (1986).
15. K. W. Kratky, *Phys. Rev. A* **31**:945 (1985).
16. K. W. Kratky, unpublished results.
17. J. J. Erpenbeck and W. W. Wood, in *Statistical Mechanics*, Part B, Bruce J. Berne, ed. (Plenum Press, New York, 1977).
18. R. Grover, W. G. Hoover, and B. Moran, *J. Chem. Phys.* **83**:1255 (1985).